# Aerodynamic Shape Optimization of a Low Drag Fairing for Small Livestock Trailers

C. A. Gilkeson[1], V. V. Toropov[2], H. M. Thompson[3], M. C. T. Wilson[4], N. A. Foxley[5], and P. H. Gaskell[6]
*University of Leeds, Leeds, West Yorkshire, LS2 9JT*

**Small livestock trailers are commonly used to transport animals from farms to market within the United Kingdom. Due to the bluff nature of these vehicles there is great potential for reducing drag with a simple add-on fairing. This paper explores the feasibility of combining high-fidelity aerodynamic analysis, accurate metamodeling, and efficient optimization techniques to find an optimum fairing geometry which reduces drag, without significantly impairing internal ventilation. Airflow simulations were carried out using Computational Fluid Dynamics (CFD) to assess the performance of each fairing based on three design variables. A Moving Least Squares (MLS) metamodel was built on a fifty-point Optimal Latin Hypercube (OLH) Design of Experiments (DoE), where each point represented a different geometry configuration. Traditional optimization techniques were employed on the metamodel until an optimum geometrical configuration was found. This optimum design was tested using CFD and it matched closely to the metamodel prediction. Further, the drag reduction was measured at 14.4% on the trailer and 6.6% for the combined truck and trailer.**

## Nomenclature

| | | |
|---|---|---|
| $L$ | = | One combined vehicle length consisting of the trailer and towing vehicle. |
| $D_1$ | = | Design variable for the radius of the fairing. |
| $D_2$ | = | Design variable for the lower edge extension of the fairing. |
| $D_3$ | = | Design variable for the frontal curvature of the fairing when viewed from above. |
| $C_d$ | = | Aerodynamic drag coefficient acting in the flow direction. |
| $Q$ | = | Air exchange rate through the lower deck of the trailer. |
| $p$ | = | Apparent order of the CFD solution. |
| $w_i$ | = | Gaussian weight decay function of the $i$th DoE point. |
| $r_i$ | = | Euclidean distance from the $i$th DoE point. |
| $\theta$ | = | Closeness of fit parameter. |
| $C_p$ | = | Pressure coefficient. |

## I.  Introduction

Continual improvements in available computing power are facilitating analysis of ever more complex problems in science and engineering. One area which has benefited enormously is Computational Fluid Dynamics (CFD). The application of CFD to vehicle aerodynamics is helping to direct design effort, resulting in successful drag reduction and aerodynamic stability improvements[1,2]. The reliability of CFD is now such that applying optimization

---

[1] PhD Student, School of Mechanical Engineering, University of Leeds, AIAA student member.

[2] Professor, School of Civil Engineering, University of Leeds, AIAA Associate Fellow.

[3] Senior Lecturer, School of Mechanical Engineering, University of Leeds.

[4] Academic Fellow, School of Mechanical Engineering, University of Leeds.

[5] PhD Student, School of Computing, University of Leeds, AIAA student member.

[6] Professor, School of Mechanical Engineering, University of Leeds.

techniques in search of the best design can offer potentially huge benefits in terms of improved fuel economy by means of drag reduction and aerodynamic shape optimization.

One important case, not been considered previously, is the design of small livestock trailers which are the primary means of transporting animals to market in the UK, Fig. 1. These trailers, which are towed by off-road vehicles such as pick-up trucks, are primarily designed with space considerations in mind. As a result, their shape is essentially a box on wheels with little or no consideration of aerodynamics. Ventilation of the internal environment is achieved passively by virtue of vehicle movement. This induces air exchange between the internal flow and the outer free-stream through a series of rectangular apertures on either side of the vehicle. In terms of animal welfare it is essential to ventilate the internal environment adequately.

The bluff nature of these vehicles induces highly separated flows and significant levels of form drag[3]. Consequently the potential gains from optimizing these trailers are significant, however this must be achieved without impairing the air exchange rates. Striking the balance between minimizing drag and maintaining ventilation is paramount when considering design changes to the trailer. The objective therefore is to find an optimum design by coupling CFD simulations with an optimization procedure.



**Figure 1.  CAD model of a typical livestock trailer towed by an off-road vehicle.**

## II.  Model Set-Up

The process of setting up a platform from which to identify an optimum trailer design involved a number of steps. Firstly, a CFD model was developed so that different geometries could be assessed to provide accurate and reliable data for drag and ventilation. Next, a region on the trailer was chosen for optimization and this was parameterized in terms of three geometric design variables. An Optimal Latin Hypercube Design of Experiments consisting of 50 points was then used as training data for a metamodel constructed using the Moving Least Squares method. Each data point involved a computationally expensive high-fidelity CFD solve for geometry composed from the three design variables. The resulting metamodel was then be refined using further CFD results to identify the optimum configuration.

**A.  CFD Model Development**

The CFD model was based upon a CAD representation of a long wheelbase Land Rover and an actual livestock trailer, Figs. 1 and 2(b). This geometry was generated from physical measurements to ensure the correct shapes were modeled. The following steps were then taken to construct the CFD model:

*1.  Solution Domain*

Due to the computationally expensive nature of this problem, a symmetry plane was used to speed up calculations. The air volume surrounding these vehicles effectively had a semi-elliptical cross section, Fig. 2(a). This gave a ground-level width of 95.2m (10*L*) and a maximum height of 38.1m (4*L*). The blockage imposed upon the flow by the vehicles was 0.2% based upon the frontal area ratio. In order to fully capture the turbulent wake behind the vehicles, a domain length of 247.5m (26*L*) was used with the wake region extending twenty vehicle lengths behind the trailer. Later analysis on this geometry established that the external boundaries (i.e. inlet, outlet and ceiling) were placed sufficiently far from the vehicles so that blockage effects did not alter the solution.
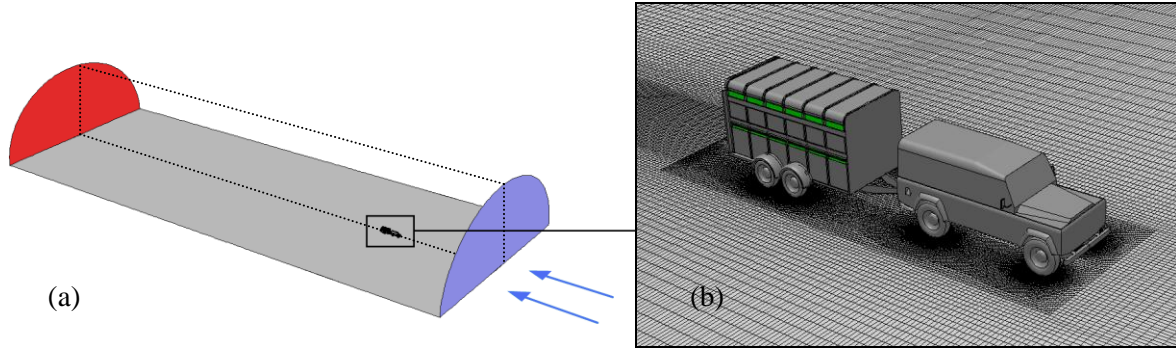
**Figure 2. Illustration showing the ground plane, the inlet and the outlet of the full solution domain i.e. reflected about the symmetry plane (a) and a close-up of both vehicles with the grid (b).**

*2. Boundary Conditions*

Air entered the solution domain through a single velocity inlet and exited through a pressure outlet at atmospheric pressure. An inlet velocity of 22.4m/s (50mph) was used and this was matched by a moving ground plane. The initial turbulence level occurring in the domain was specified in terms of the turbulence intensity which was set at 0.25% and the turbulent length scale which is defined as 7% of the characteristic length, giving a value of 0.66m. Moving boundaries were implemented on the wheels for each vehicle with appropriate rotational velocities. Wall-type boundary conditions were used on the surfaces of the vehicles in conjunction with standard wall functions to treat the near-wall regions.

*3. Grid Structure*

Decomposition of the solution domain was essential to generate a grid which adequately represented the geometry. The air volume was split longitudinally into two distinct zones resulting in a core region and an adjacent shell spanning the entire length of the domain. This allowed use of a 'C' type grid in the shell which contained 0.9 million hexahedral cells (all cell counts are quoted for the half domain). The core region was further decomposed into three zones which permitted 0.1 million prism cells to be used upstream of the vehicles and a further 1.0 million cells downstream.

Within the remaining central core, the fluid was decomposed inside the trailer such that structured hexahedral cells filled the internal air volume. A boundary layer mesh containing 12 layers of cells and a thickness of 80mm was used on the primary surfaces of the trailer which consisted of the side panel, the roof and the headboard, Fig. 3(a) and (b). Due to the relative complexity of the other geometrical features (i.e. wheels and underbody components) it was necessary to make use of an unstructured tetrahedral grid to fill the remaining space within this central core.

*4. Verification*

An important aspect of any CFD modeling process is to establish the extent to which the solutions being obtained are dependent on the grid density[4]. A grid independence study was carried out which involved successively refining all the cells within the central core with particular attention paid to the internal air volumes and the external boundary layer grid. The one-equation Spalart-Allmaras turbulence model was used in the simulations since results based on this model have been found to compare well with wind tunnel experiments for a similar problem[3]. Three grids were generated with cell counts of 5.2 million, 6.7 million, and 8.1 million. The resulting solutions were assessed in terms of the drag coefficient, $C_d$, and the air exchange rate passing through the lower deck of the trailer, $Q$, Table. 1.

These solutions exhibited oscillatory convergence with an apparent order, $p$, of 2.38 which was consistent with the hybrid second order/QUICK discretization scheme used. Solution errors between the medium and fine grid were calculated using the well established Grid Convergence Index (GCI)[4]. Errors were predicted at 1.5% for the drag coefficient, and 2.0% for the air exchange rate. On the basis of these findings, the medium grid density of 6.7 million cells was used in subsequent simulations.
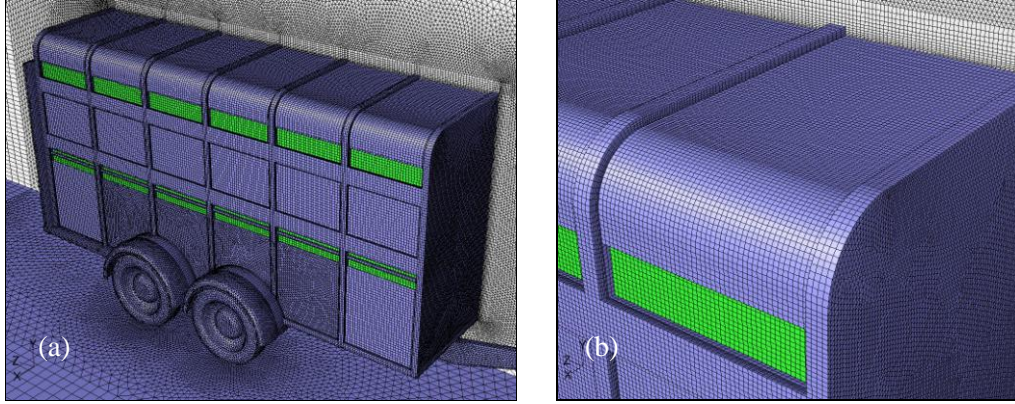
**Figure 3. Illustration showing the general grid structure surrounding the baseline configuration (a) with a close-up of the boundary layer elements (b).**

| Grid Type | Cell Count | $C_d$ | $Q$ (m$^3$/s) |
|---|---|---|---|
| Coarse | 5207258 | 0.5414 | 0.2965 |
| Medium | 6669465 | 0.5376 | 0.2943 |
| Fine | 8076558 | 0.5441 | 0.2976 |
| Ideal | $\infty$ | 0.5507 | 0.3024 |

**Table 1. Solutions generated on the baseline model for different grid densities vs. the ideal 'zero grid-spacing' based on the Grid Convergence Index.**

## B. Optimization Methodology

Having developed a procedure for obtaining accurate CFD results, the next stage was to integrate this with an optimization method such that an optimum design could be found.

### 1. Design Variables and Objective Function

Initial results from the baseline configuration (i.e. the standard trailer case) showed that 39% of the total trailer drag acted on the headboard, with 34% attributable to the tailboard and the remaining 27% belonging to the wheels and other minor surfaces. When considering the best location for a drag-reducing fairing, clearly a shape optimized headboard fairing offers the greatest potential and such a device would not interfere with day-to-day trailer operation.

In previous studies this type of device has been successful in reducing drag[5,6] whilst more generic bluff-body drag reduction has shown that the magnitude of edge radii plays a significant role[7-9]. With this in mind the fairing was parameterized in terms of three design variables, namely the side radius, $D_1$, the lower edge extension, $D_2$, and the central extension of the fairing, $D_3$, Fig. 4. Effectively $D_2$ dictates the rake angle of the device whilst $D_3$ determines the level of curvature in the fairing when viewed from above. In order for the fairing to integrate successfully with the existing trailer, $D_1$ and $D_2$ were both assigned a range of 175-600mm, with a smaller range of 0-200mm for $D_3$.

The objective function to be minimized was the drag coefficient for the two vehicles combined. Previous work has indicated that ventilation on the lower deck is significantly less than that observed on the upper one[3]. Hence a decision was taken to ensure that any minimum-drag design would not be considered for analysis if the air exchange rate on the lower deck was reduced by more than 30%.
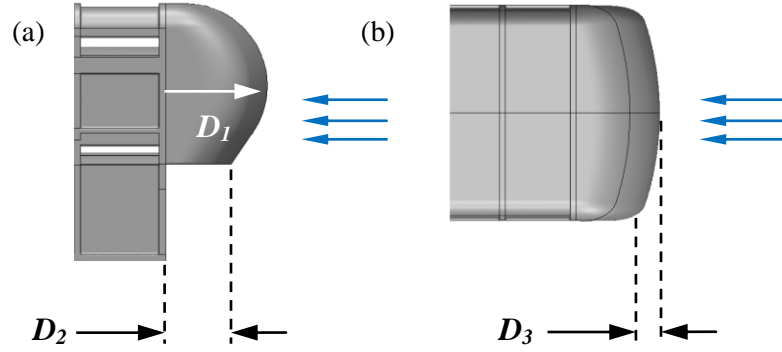
**Figure 4. Illustration of the three design variables shaping the headboard fairing. Side view (a) and aerial view (b).**

*2. Design of Experiments*

An Optimal Latin Hypercube (OLH) Design of Experiments (DoE)[10] was employed to fill the parameter space with 50 different fairing designs using combinations of $D_1$, $D_2$, and $D_3$. The DoE was divided into two parts, a 40-point model building DoE and a 10-point model validation DoE. By configuring the DoE in this way, the metamodel could be built on the first DoE and validated on the second, before being rebuilt on the merged 50-point DoE. A specific feature of this approach is that all three DoE's (model building, model validation and the merged one) are space-filling and uniform[10].

The input parameters corresponding to each DoE point were used to systematically generate a CAD model and the corresponding mesh file for each fairing design. Figure 5 shows three fairings of the fifty required to construct the metamodel.
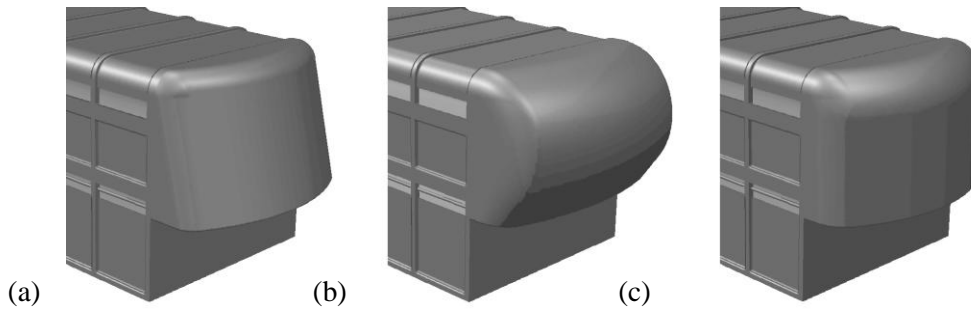


**Figure 5. Illustration of three headboard fairings based on parameter sets from the DoE.**

*3. Metamodel*

CFD post-processing carried out on all 50 fairing designs provided the responses for the metamodel building, which in this case was based on the MLS method[11] with a quadratic base function and a Gaussian weight decay function, $w_i$, Eq. (1).

$$w_i = exp(-\theta r_i^2) \tag{1}$$

The parameter $r_i$ is the Euclidean distance from the $i^{th}$ DoE point whilst $\theta$ denotes the user defined "closeness of fit" parameter. For the specific case of $\theta = 0$, the MLS approximation reduces to conventional least squares polynomial response surface fitting. Otherwise, the value of $\theta$ can either be specified *a priori* or optimized to produce the best fitting metamodel for the given training data.

The metamodel itself was built using a three stage process. An initial metamodel was constructed from the 40-point build DoE and the corresponding CFD response values. The 10-point validation DoE then acted as a guide for tuning $\theta$ to minimize the RMS error between the metamodel prediction and the CFD responses at the validation locations. Finally, the optimal value of $\theta$ was used to re-build the metamodel on the 50-point merged DoE and the associated CFD responses. The validation DoE also served to validate the initial metamodel to ensure adequate accuracy, thereby ensuring the accuracy of the final metamodel.

## III.   Results

Following the development of the numerical model, a high fidelity CFD solve was computed for each of the fairing designs specified by the DoE. The resulting CFD response values were then fed into a commercial optimization package to construct the metamodel. This metamodel was optimized to search for the best design, which was tested using CFD to validate the prediction. Comparisons between the aerodynamic characteristics of the optimum design and the baseline case were then considered.

### A.  CFD Solutions

A CAD model for each of the 50 headboard fairing designs generated by the DoE was created using the commercial package Gambit (version 2.3). Each grid was constructed with the same density as that of the medium grid discussed in the previous section, resulting in cell counts of ~ 6.6 million for all models.

Solutions were obtained using a steady-state approach to the problem since a time-dependent formulation, though desirable, would take an order of magnitude longer which was not feasible given the time available. Residual histories showed that solution convergence occurred between 8500 and 9000 iterations but each simulation was run for a total of 10000 to avoid convergence error. Typically, run times of 72 hours were seen using an arrangement of four processors in parallel. Once the simulations were set up, all fifty solutions were generated in approximately 4 weeks with the computational resources available. The computations were carried out with the commercial CFD code, Fluent (version 6.3). Analysis of the solutions showed that the drag force acting on the truck-trailer reduced every time, compared with the baseline model.

### B.  Optimization Procedure

The most important aspect of the whole exercise was to construct a reliable metamodel from which to find the optimum fairing design. Altair's commercial package, HyperStudy (version 8) was employed for this purpose. Having generated the metamodel using the three stage technique described above (build–validate–rebuild), traditional optimization techniques were employed to find a design for minimum drag. This was achieved in two stages. Firstly, a Genetic Algorithm (GA) containing 20 individual chromosomes was applied to the metamodel to search for the global minimum. This was performed several times with different initial populations until the termination criteria were attained. Each time termination occurred within 25 iterations and very similar design predictions were made, thus increasing the likelihood that the global optimum had been identified. Secondly, a gradient method, namely the Sequential Quadratic Programming (SQP) technique was used to 'home in' on the global minimum for $C_d$. No change in the predicted design was found but this was probably because the corner point of the design space had been located.

### C.  Aerodynamic Analysis

The minimum-drag fairing design predicted by the metamodel was composed of the greatest values of $D_1$, $D_2$, and $D_3$ within the design space. This geometry was tested using the CFD model and the result was within 0.4% of the metamodel prediction, highlighting the reliability of the whole process. To ensure that the optimum had been correctly identified, the extra point was added to the merged-DoE to refine the metamodel. Optimization on this updated metamodel made no difference to the predicted optimum, and so this fairing design could be analyzed in more detail with confidence.

### 1. *Drag Comparison*

The optimum fairing design reduced drag on the trailer by 14.4% but conversely it increased by 9.1% on the towing vehicle. However the net effect was a drag reduction of 6.6% for the combined vehicles compared with the baseline case, Table. 2. The strong performance of this design is evident in Fig. 6 which shows a plot of the drag coefficient against the percentage reduction in flow rate for all 51 CFD results. Equally as important is the fact that the air exchange rate is only reduced by 11.1% over the baseline, which is well within the previously mentioned limit of 30%

| | Drag Force (N) | | |
| --- | --- | --- | --- |
| | Baseline | Minimum Drag Design | Difference (%) |
| Truck | 165.2 | 180.4 | +9.1 |
| Trailer Headboard | 106.5 | 65.5 | -38.5 |
| Trailer Tailboard | 94.5 | 98.9 | +4.6 |
| Trailer Wheels + Arches | 27.3 | 29.8 | +9.3 |
| Trailer Other | 47.8 | 37.6 | -21.3 |
| Total | **441.3** | **412.2** | **-6.6** |

**Table 2.   Detailed comparison of the drag contributions for the baseline and minimum drag designs.**
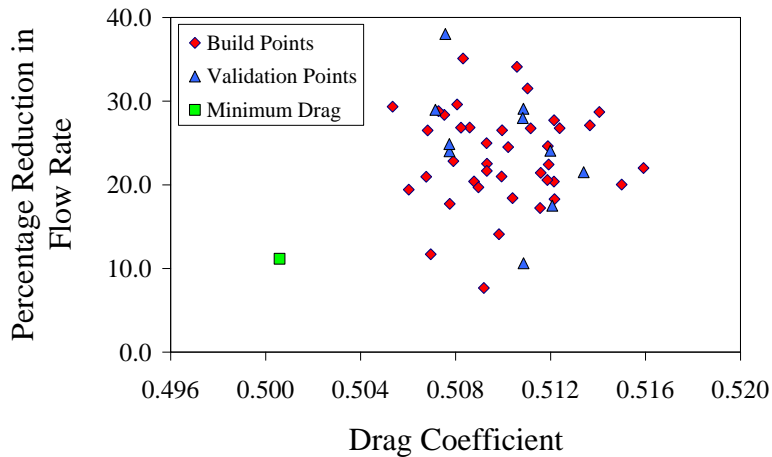


**Fig 6.  Plot showing the CFD results obtained from the build and validation DoE's and the minimum-drag design.**

### 2. *Pressure Distributions*

The single largest benefit came from the headboard and this occurred due to the surface pressure distribution. The high-pressure stagnation region was reduced in size (red area) and this was accompanied by a smaller low-pressure area immediately behind it (blue region), Fig. 7. Both of these effects indicate that the pressure gradients were smaller, which is a typical characteristic of reduced drag. The reason why ventilation was slightly poorer is that the low pressure area migrated away from the rectangular vent apertures to the upper surface and shoulders of the fairing, Fig. 7. Consequently, the usual suction force which extracts air from the interior had moved too far away from the apertures to have as large an effect on the ventilation.
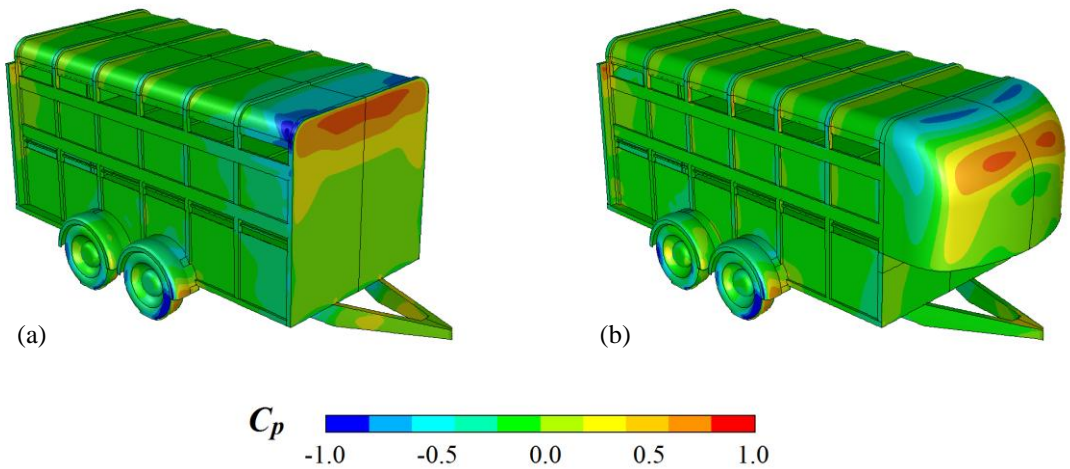
American Institute of Aeronautics and Astronautics

**Figure 7. Surface contour plots of the pressure coefficient, $C_p$, for the baseline trailer (a) and the minimum drag fairing predicted by the metamodel (b).**

*3. Airflow Patterns*

The oil-flow plots shown in Fig. 8 highlight the differences in the airflow patterns close to the surfaces of the trailer. Although there is little difference along the side panels, the flow passing over the roof of the minimum-drag design is laminar in nature and structured, whereas separation and flow reversal is evident on the standard trailer.
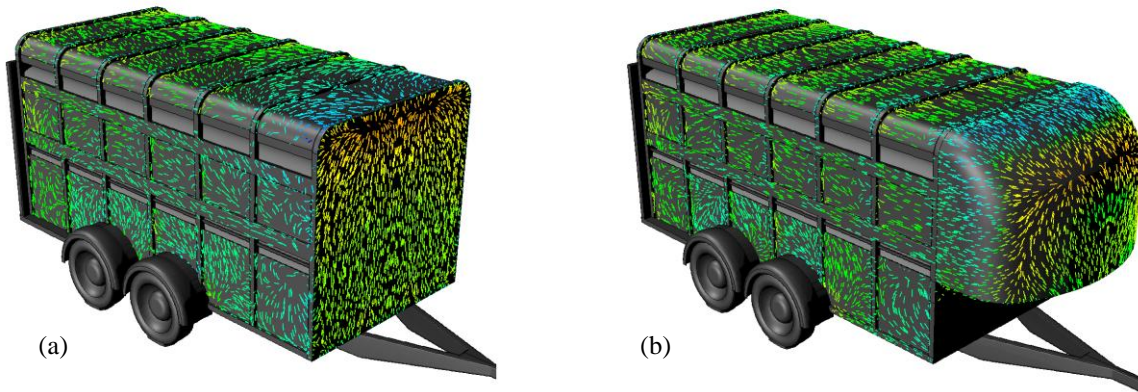


**Fig 8. Oil flow plot for the baseline model (a) and the modified trailer together with the minimum-drag fairing (b).**

Moving away from the surfaces of the trailer, the external flow field was visualized by releasing a total of 230 seeds from a vertical plane located 0.1m behind the base of the truck. In each case these seeds were carried with the flow, Fig. 9. The most striking feature from the baseline case is the significant level of recirculation within the towing gap, which leads to a large trapped vortex structure occurring in the void. Some of this is ejected into the free-stream resulting in a column of air passing above the wheel arches, Fig. 9(a).

For the minimum drag case, the presence of the fairing forces the majority of the air to flow above and below the trailer, with a much smaller volume moving past the side panels, Fig. 9(b).

It would appear that the fast-moving air flowing beneath the two vehicles tends to pull the seeds down and through the much smaller towing gap, eventually dispersing them in the wake of the trailer. So effectively, with the fairing in place, the wake of the towing vehicle is redistributed within the trailer wake with noticeably less side spillage. Thus the new headboard is instrumental in controlling the airflow downstream.
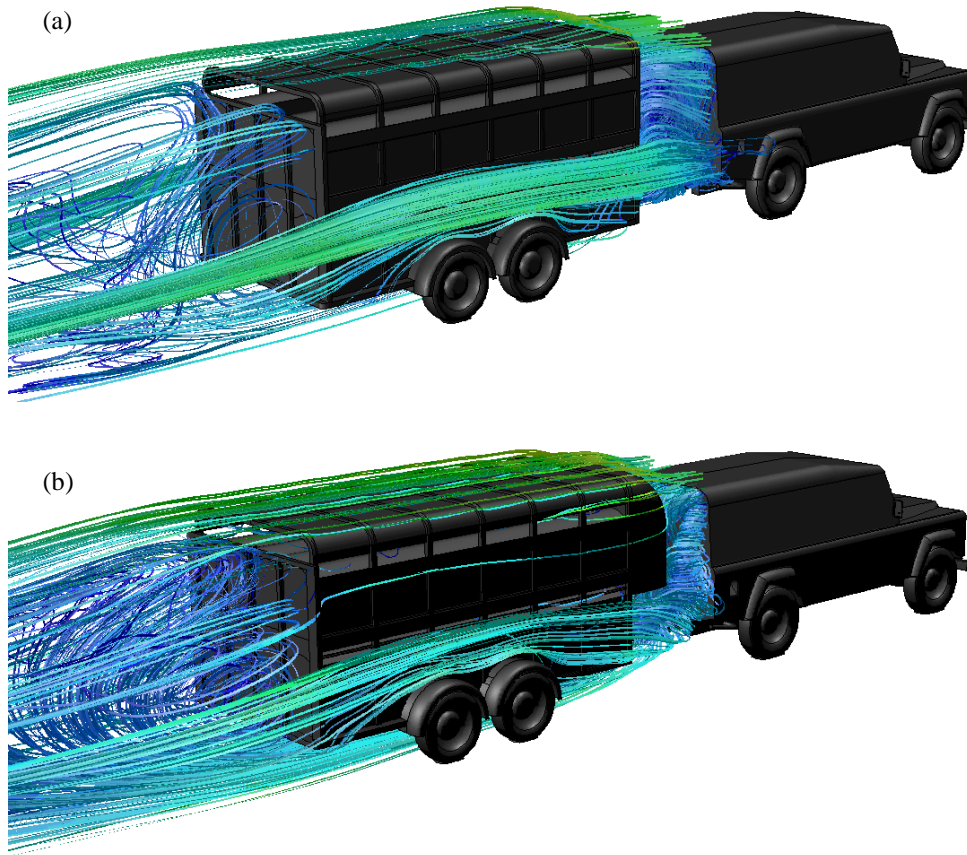


**Fig 9. Pathlines generated by seeds released from a plane immediately behind the truck for the baseline trailer (a) and the modified trailer (b).**

## IV.  Discussion

The purpose has been to establish whether the concept of aerodynamic shape optimization is feasible when combining the strengths of CFD and the MLS method. This strategy worked extremely well in optimizing a livestock trailer and the resulting drag reduction of 6.6% can be considered a success. Past studies documenting fuel consumption for heavy vehicles have shown that significant amounts of fuel can be saved by fitting drag-reducing fairings[12]. On the basis of these data and a drag reduction figure of 6.6%, fuel savings of approximately 2.5% could be expected for the chosen design.

The success of this investigation was due to a number of factors. Firstly, the design variables were carefully chosen to replicate well-established practices such as using large radii. Hence known solutions were inherent in the model set-up, which undoubtedly aided the final outcome. In fact, the optimum fairing design was the largest, most bulbous shape possible within the design space. From an aerodynamic viewpoint, this solution is by far the most intuitive of the possible designs. Larger shapes with more progressive contours generally induce smaller local pressure gradients, which in turn minimize flow separation and hence drag. One criticism of this could be that the

problem was formulated in a manner which was too conservative, eliminating the possibilities for more adventurous and less-intuitive solutions.

However, common sense dictates that a more conservative problem formulation can clearly assess whether the technique has any merit. Further, there were practical restrictions when generating the CAD models which meant that relatively simple rules had to be followed.

Another factor which led to the final result was the quality of the CFD modeling. A significant amount of time was dedicated to the development of the CFD process. Every possible step was taken to minimize the errors in the solutions. Double precision real-number representation reduced round-off error and simulations were run for long enough to ensure that convergence error was minimized. Discretization errors were estimated using the Grid Convergence Index as part of a grid independence study and they were found to be small. Care was taken to mesh the models with as many structured cells as possible so that the effects of numerical diffusion were limited. In addition, a boundary layer grid on the main surfaces of the trailer was employed to correctly model near-wall turbulence, thus providing the best information for calculating accurate drag values.

Although the class of turbulence model used was robust and reliable, its formulation is steady-state in nature. An interesting future investigation would be to adopt a time-dependent turbulence modeling approach such as Large Eddy Simulation (LES) to capture effects including vortex shedding. However, this cannot be done with a symmetry plane in place and the computational effort would be vastly greater than that required to generate the present solutions.

Clearly, the MLS metamodel worked exceptionally well in fitting through the DoE points to find the optimum design, which was later validated by the CFD model. Generally speaking, there are several accepted methods for generating metamodels such as Sheppard Weighting Functions (SWF), Radial Basis Functions (RBF), Kriging and MLS[13,14]. However, interpolation techniques such as RBF and Kriging can force the surrogate hypersurface into unnatural behavior, particularly when fitting to noisy data[15]. Approximation techniques such as MLS are inherently smoother since they do not necessarily pass through each response value. One reason why the MLS approximation was used to construct the metamodel was that the closeness of fit parameter embedded in the weight decay function, allowed for small errors in the responses. From the results obtained, this method worked extremely well for this application.

The most obvious future development of this work will be to investigate how well the technique copes with multi-objective optimization, as for non-trivial engineering applications it is highly likely that more than one objective function would need to be optimized.

## V.  Conclusion

Aerodynamic shape optimization has been applied to a small livestock trailer fairing using an MLS metamodel in combination with CFD. The fairing was parameterized in terms of three design variables. A 50-point DoE was used to set up a series of high-fidelity CFD solutions with aerodynamic drag being the objective function. The metamodel was constructed using these solutions and then optimized through traditional optimization techniques, which succeeded in finding an optimum design. One final CFD solution verified that the metamodel was accurate. The optimum design succeeded in reducing drag by a margin of 6.6%. The air exchange rate on the bottom deck of the trailer was 11.1% less than that of the baseline. However, this value was well within the specified limit of 30% reduction. On the basis of this result, it can be concluded that CFD and the MLS method combined well for this particular application.

# References

[1]Caldirola, L., Cannizzo, G., Petrotta., "The Aerodynamic Development of the Ferrari FXX," *Proceedings of the 6th International Vehicle Aerodynamics Conference*, Gaydon, UK, 2006, pp. 22-33.

[2]Lock, A. S., "Computational Fluid Dynamics Development of the JCB Dieselmax Land Speed Record Vehicle," *Proceedings of the 6th International Vehicle Aerodynamics Conference*, Gaydon, UK, 2006, pp. 34-46.

[3]Gilkeson, C. A., Wilson, M. C. T., Thompson, H. M., Gaskell, P. H., Barnard, R. H., Hackett. K. C., Stewart, D. H., "Ventilation of Small Livestock Trailers," *Proceedings of the 6th International Vehicle Aerodynamics Conference*, Gaydon, UK, 2006, pp. 138-147.

[4]Roache, P. J., "Quantification of Uncertainty in Computational Fluid Dynamics," *Annual Review of Fluid Mechanics,* Vol. 29, 1997, pp., 123-160.

[5]Garry, K. P., "Development of Container-Mounted Devices for Reducing the Aerodynamic Drag of Commercial Vehicles," *Journal of Wind Engineering and Industrial Aerodynamics,* Vol. 9, 1981, pp., 113-124.

[6]Charwat, A. F., "Wind-Tunnel Study of an Add-on Streamlining Bubble on the Aerodynamics of Utility Box-Trailers," *Journal of Wind Engineering and Industrial Aerodynamics,* Vol. 11, 1983, pp., 431-440.

[7]Cooper, K. R., "The Effect of Front-Edge Rounding and Rear-Edge Shaping on the Aerodynamic Drag of Bluff Vehicles in Ground Proximity," *Society of Automotive Engineers,* Paper No. 850288, 1985.

[8]Hucho, W. H., *Aerodynamics of Road Vehicles*, 4th ed., SAE International, 1998, Chap. 9, pp., 449-452.

[9]Barnard, R. H., *Road Vehicle Aerodynamic Design,* 2nd ed., MechAero Publishing, 2001, Chap. 5, pp., 104-108.

[10]Narayanan, A., Toropov, V. V., Wood, A. S., Campean, I. F., "Simultaneous Model Building and Validation with Uniform Designs of Experiments," *Engineering Optimization*, Vol. 39(5), 2007, pp., 497-512.

[11]Toropov, V. V., Schramm, A., Sahai. A., Jones, R., Zeguer, T., "Design Optimization and Stochastic Analysis Based on the Moving Least Squares Method," *6th World Congress of Structural and Multidisciplinary Optimization*, Rio de Janeiro, Brazil, May 2005, CD-ROM Proceedings, eds.: Herskovits, J., Mazorche, S., Canelas, A.

[12]Rose, M. J., "Commercial Vehicle Fuel Economy – The Correlation Between Aerodynamic Drag and Fuel Consumption of a Typical Truck," *Journal of Wind Engineering and Industrial Aerodynamics,* Vol. 9, 1981, pp., 89-100.

[13]Jones, D. R., "Taxonomy of Global Optimization Methods Based on Response Surfaces," *Journal of Global Optimization,* Vol. 21, 2001, pp., 345-383.

[14]Simpson, T. W., Mauery, T. M., Korte, J. J., Mistree, F., "Comparison of Response Surface and Kriging Models for Multidisciplinary Design Optimization," *AIAA-98-4755,* 1998.

[15]Forrester, A. I. J., Keane, A. J., Bressloff, N. W., "Design and Analysis of "Noisy" Computer Experiments," *AIAA Journal,* Vol. 44, No. 10, 2006, pp., 2331-2339.